International Journal on Artificial Intelligence Tools

NAVIGATION OF AN AUTONOMOUS SEWER INSPECTION ROBOT BASED ON STEREO CAMERA IMAGES AND LASER SCANNER DATA

ALIREZA AHRARY[1,3], LI TIAN[2], SEI-ICHIRO KAMATA[2] and MASUMI ISHIKAWA[3]
[1] *FAIS-Robotics Research Institute*
2-1 Hibikino, Wakamatsu-ku, Kitakyushu 808-0196, Japan
[2] *Graduate School of Information, Production and System, Waseda University*
2-7 Hibikino, Wakamatsu-ku, Kitakyushu 808-0135, Japan
[3] *Graduate School of Life Science and Systems Engineering, Kyushu Institute of Technology*
2-4 Hibikino, Wakamatsu-ku, Kitakyushu 808-0196, Japan
ali@ksrp.or.jp, tianli@ruri.waseda.jp, kam@waseda.jp, ishikawa@brain.kyutech.ac.jp

Received (Day Month Year)
Revised (Day Month Year)
Accepted (Day Month Year)

Sewer environment is composed of cylindrical pipes, in which only a few landmarks such as manholes, inlets and pipe joints are available for localization. This paper presents a method for navigation of an autonomous sewer inspection robot in a sewer pipe system based on detection of landmarks. In this method, location of an autonomous sewer inspection robot in the sewer pipe system is estimated from stereo camera images. The laser scanner data are also used to ensure accurate localization of the landmarks and reduce the error in distance estimation by image processing. The method is implemented and evaluated in a sewer pipe test field using a prototype robot, demonstrating its effectiveness.

Keywords: Autonomous; sewer inspection; robot navigation; stereo matching; laser scanner; sewer pipe system.

1. Introduction

Pipe walls in sewer systems are prone to be damaged due to aging, traffic and chemical reactions, causing rainwater and groundwater seep into pipe systems. Regional city government reports[1] state that this inflow amounts to approximately 30 percent of the total water flow. In addition to the inflow, outflow from damaged systems also occurs, contaminating the surrounding environment[2−4].

Currently, inspection is carried out using a cable-tethered robot with an onboard video camera system. An operator remotely controls the movement of the robot and the video system. By this video-supported visual inspection, any noticeable damages or abnormalities are recorded. The reliability of this system depends on the experience of an operator. Therefore, the current manual inspection system is tedious and erroneous.

To ameliorate this difficulty, an autonomous and real-time sewer inspection robot is desired for identifying and extracting faulty areas. One of the central issues in developing an autonomous sewer robot is its navigation. Detecting landmarks such as manholes, inlets and joints in a sewer pipe system is an important task in navigation. In this paper, we propose a method for detecting landmarks and estimating the location of a mobile robot based on stereo camera images and laser scanner data.

Various methods have been proposed for the detection of landmarks. Hertzberg and Kirchner conducted experiments on navigation of a sewer robot in a dry sewer test field at GMD, Sankt Augustin[5]. They succeeded in detecting local features by ultrasonic sensors. The detected landmarks were then scanned by a different, pivoted ultrasonic transducer. Finally, local features obtained by the scanner are classified using a specially trained artificial neural network. Although this method has a high rate of classification (75 out of 81 samples), it lacks the capability of locating an individual manhole.

Schonherr et al.[6] proposed a pivoted ultrasonic transducer that permanently scans the walls of the upper half section of pipes for detecting inlet. This procedure is time consuming. Paletta et al. proposed a method for detecting inlets from grayscale images taken by an onboard CCD camera[7]. Although it involves a time consuming training phase, the detection of inlets by trained neural networks is fast.

In a real sewer pipe system, a robot is required to explore unknown sewer area during the training phase. This property of time consuming training is undesirable from a practical point of view. To automatically detect damages in sewer pipes, Campbell et al.[8] and Clarke[9] proposed pipe profiling methods for 3D reconstruction. Using sensor devices mounted on a teleoperated sewer robot, data evaluation is performed in a stationary surveillance vehicle.

Our method uses stereo camera images and laser scanner data for detecting landmarks. A sewer inspection robot is capable of self localization, which is impossible by the above methods. In our method, the stereo images are captured by a stereo camera at the front of a robot. A fast and accurate stereo matching measure named a linear computation (here after referred to as LC) computes the distance between a sewer inspection robot and a landmark based on the stereo images. We refine the distance by a threshold elimination function. If the distance is less than 10cm, we check laser scanner data to detect the exact location of the landmark. Finally, information on the locations of a robot and landmarks are used for robot navigation.

The paper is organized as follows. Section 2 gives overview of our sewer pipe system. Then we present our method in detail in Section 3. Section 4 shows experimental results by our method. Section 5 provides conclusions.

2. Sewer Pipe System

Sewers mainly consist of smooth, uniform cylindrical or elliptical pipes. Fig. 1 illustrates the sewer pipe construction with the manhole over each pipe-bend, the inlets from houses, and the joints conecting two pipes.

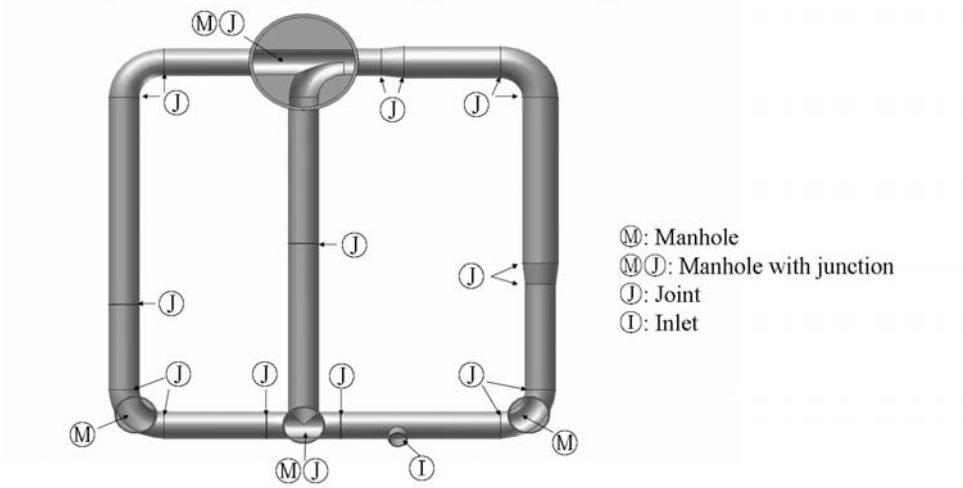

Fig. 1. Landmarks in the sewer pipe system.

For navigation in a sewer pipe system, a robot needs distinctive landmarks. Elements like manholes, inlets and pipe joints are well suited for this purpose. As shown in Fig. 2, manholes are always located in the upper part of the sewer image, while joints and inlets are always in the centeral and upper half of the sewer image. This facilitates the extraction of their positions from the image. The fact that the maximum length of a plastic or ceramic pipe is less than 2m makes capturing landmarks still easier. The resulting map has descriptions on manholes, inlets, pipe joints, the distance between them and so forth.

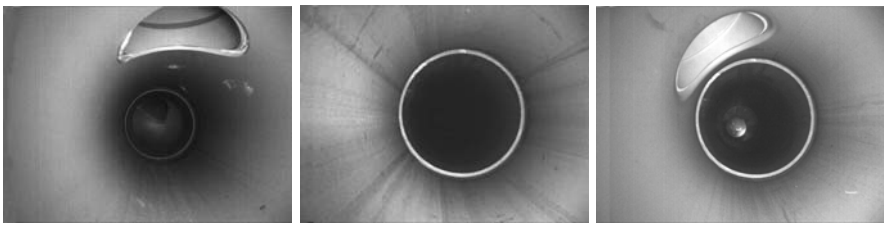

(a) The manhole. (b) The joint. (c) The inlet.

Fig. 2. Locations of the landmarks in the sewer images.

2.1. *The autonomous sewer inspection robot, KANTARO*

In the conventional sewer inspection, commercially available robots are capable of moving inside of straight pipes, but not capable of passing through pipe-bends such as "curves", "joints" and "T-junctions." Therefore, the design of a robot capable of moving inside of straight pipes and passing through pipe-bends is expected to bring great progress in sewer inspection industry.

We have designed a compact and novel moving mechanism for sewer inspection robots. The design is based on passive adaptation of robot wheels to the bends in the pipe. This is accomplished by proper adjustment of wheel orientation and passive damping of springs. A single robot with this new moving mechanism can load a controller, electronic devices, motors and sensors, and is capable of passing through any pipe bends, moving inside of different sized pipes and avoiding obstacles without intelligent control using sensors. Fig. 3 shows the overview of the prototype autonomous sewer inspection robot, KANTARO[14].

Fig. 3. The prototype autonomous sewer robot, KANTARO.

2.2. *Vision system*

Our sewer inspection robot is designed for checking a sewer pipe system based on sensory data such as stereo camera images and laser scanner data. Obtained data on the sewer system can be used for inspection and navigation. The environment in the pipe is less affected by changes of external light. Lighting condition is controlled by an array of white LEDs around the camera to acquire the best quality image.

2.3. *Laser scanner*

It is difficult to use the conventional laser scanner on mobile robots such as KANTARO because of its size and weight. Therefore, we design the new laser scanner in

Fig. 4 for Kantaro. The sensor is mounted on the rear-center of KANTARO and IR beam is emitted from the top of a rotary segment. The microcontroller calculates the distance, the laser scanner angle and so on. Data are transmitted to a computer at the sampling speed of 10KHz via the network with the maximum transmission rate of 1Mbps. Fig. 5 illustrates the errors in distance measurement. Table 1 describes the specification of the 2D laser scanner.

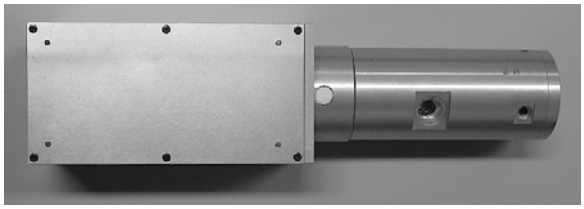

Fig. 4. The newly developed laser scanner.

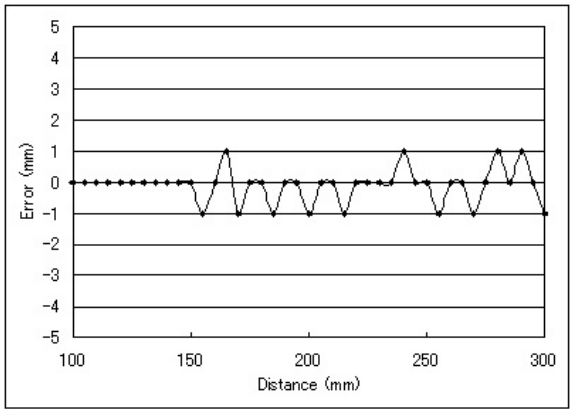

Fig. 5. Errors in distance measurement.

The diameter of the typical manhole is larger than that of the connected pipe by 50 cm, and inlet size is between 10 and 15 cm. Sewer landmarks are not uniformly distributed along the pipe perimeter. Rather, they appear in the upper part, left side and right side of pipes. This allows to restrict the search to the angle width of 15 degrees for each candidate as shown in Fig. 6, and to design the size and position of each scanning window. By full rotation of the laser scanner, the mirror rotates 360 degrees and the distance is measured at the right, top and left scanning windows.

Table 1. Specification of the Laser Scanner.

Scanning directions	360 degree
Scanning speed	0-1800 (rpm)
Distance range	70-190 (mm)
Accuracy	±1 (mm)
Beam radius	0.5 (mm)
Transmission method	Full duplex serial transmission (2Mbps)
Sampling speed	More than 10 KHZ
Measured signals output	Distance, Scanning angle
weight	200 g
Size	37 × 48 ×166 (mm)
Power	±12V(0.5A) +5V(1A)

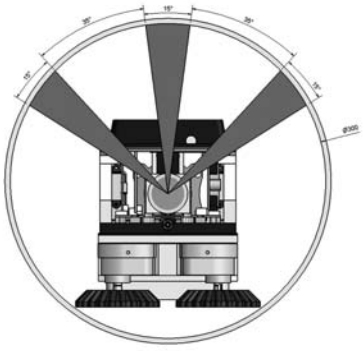

Fig. 6. Scanning directions.

3. Methodology

The proposed method in Fig. 7 is composed of two stages: estimation of the location of a mobile robot and detection of landmarks. Firstly, a stereo sewer image is captured by the stereo camera on KANTARO. Secondly, we extract two rectangular Region of Interest(ROI) images for the manholes, inlets and joints, and detect edges in each ROI image (3.1). Thirdly, a fast and accurate stereo matching measure (LC) is applied to these ROI images to estimate the distances between the robot and landmarks (3.2). Fourthly, we refine the estimated distances using a threshold elimination function (3.3). If the refined distance is less than 10cm, we check the laser scanner data to detect the landmark. Finally, the refined estimates of location of the robot and the landmarks are used for navigation (3.4).

3.1. *Edge detction in extracted Rectangular ROI Image*

In sewer pipe systems, manholes, inlets or joints are always located in particular parts of the sewer image; the manholes and inlets are always in the upper part of the sewer image, and the joints are always in the central part of the image. Fig.

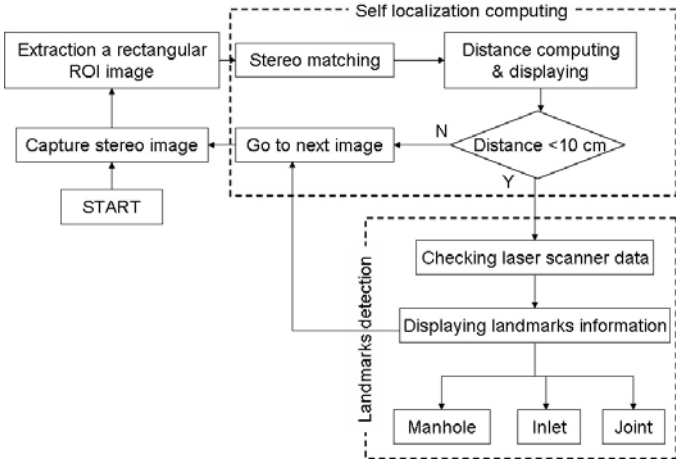

Fig. 7. Overview of the proposed method.

8 illustrates the original image and the extracted rectangular ROIs of manholes, inlets and joints.

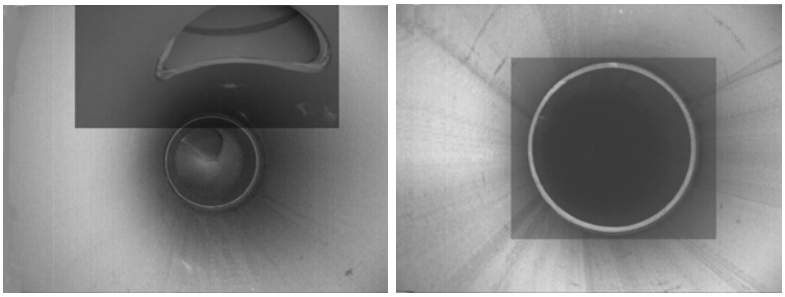

Fig. 8. Original image and the extracted rectangular ROI images. (a) The rectangular ROI image for the manhole and inlet. (b) The rectanglular ROI image for the joint.

After the extraction of ROI, we use the canny edge detector to get the edges in ROI. The Canny edge detection algorithm[13] is known to be the optimal edge detector in terms of error rate. It introduced two kinds of threshold for the gradient with hysteresis, i.e., the lower threshold T_1 and the higher threshold T_2. The values of the threshold are determined based on the following requirements. The first requirement is that edges in images should not be overlooked and that non-edges should not be detected as edges. The former corresponds to the error of the second kind, and the latter corresponds to the error of the first kind in mathematical statistics. The second requirement is that the edges be well localized. In other words, the distance between the detected edge and the actual edge be minimum. The third requirement is to produce only one response to each edge. This is included because

the first two are not enough to eliminate multiple responses to an edge.

Based on these requirements, the canny edge detector firstly filters the image to eliminate noise. It then finds the image area with large spatial derivatives. The algorithm then tracks along these regions and any pixel in an edge list with the gradient larger than the higher threshold is classified as a valid edge. Pixels connected to a valid edge and with the gradient larger than the lower threshold are also classified as an edge. The small value of the higher threshold tends to increase the number of spurious and undesirable edge fragments, hence should be avoided.

3.2. *Distance measurement by stereo matching*

An application of the conventional gradient measure for stereo matching[11] to our sewer image generates disparities, which provide the distance map based on the geometry of stereopsis[12]. The resulting distance map is represented by the brightness of pixels; the larger the distance is, the darker the pixel is. Due to the shadow, however, the conventional gradient measure tends to produce fringes of the feature pixels in the distance map as in Fig. 9.

To overcome this difficulty, we propose a new measure[10] which is partly similar to the conventional gradient measure. To compare locations in two images, most existing methods depend on *similarity* reflecting the resemblance of the corresponding locations of two images, and sometimes on *distinctiveness* reflecting the likelihood of the correctness of the match[15]. Our measure combines the similarity and the distinctiveness into a single measure of matching. Since only the horizontal shifts need to be considered in the stereo matching, the differences of the brightness between horizontally neighboring pixels are calculated. The differences between two neighboring pixels in left-eye and right-eye images are $D_L(x,y) = I_L(x,y) - I_L(x-1,y)$ and $D_R(x,y) = I_R(x,y) - I_R(x-1,y)$, respectively.

We calculate the sum of their absolute values, $C_d(x,y) = |D_L(x,y)| + |D_R(x+d,y)|$, to represent the distinctiveness, and the minus of the absolute value of their difference, $-G_d(x,y) = -|D_L(x,y) - D_R(x+d,y)|$, to represent the similarity at the displacement, d. We define the matching measure as the sum of these two terms: $E_d(x,y) = C_d(x,y) - G_d(x,y)$. In summary, for a given displacement, d, the matching measure, E_d, is:

$$E_d(x,y) = |D_L(x,y)| + |D_R(x+d,y)| - |D_L(x,y) - D_R(x+d,y)| \qquad (1)$$

To find the best match for an isolated pixel, we maximize E_d with respect to d under consideration. It is not hard to understand why our method generates strong responses at the feature pixels. If the matching pixel is a non-feature one, the difference of brightness between horizontally neighboring pixels is small. As a result, both $D_L(x,y)$ and $D_R(x+d,y)$ have small values. Hence, E_d also has a small value. On the contrary, if the matching pixel is a feature one, it has a large difference of brightness horizontally. This will result in a large value of E_d. Therefore, this method is expected to work well in the matching of feature pixels.

Int'l. Journal on Artificial Intelligence
Tools, To appear in 2007
June 30, 2006 18:54 WSPC/INSTRUCTION FILE Manuscript

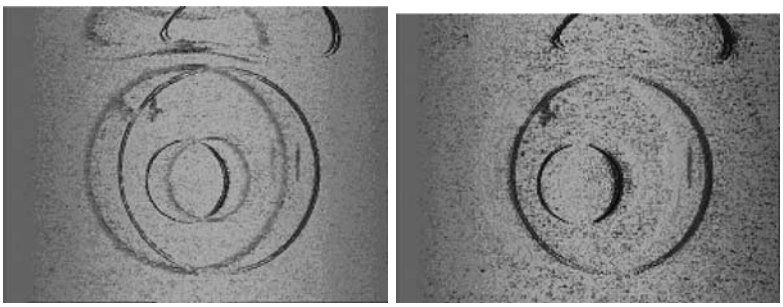

Fig. 9. Distance maps obtained by, (a) Gradient method. (b) LC method.

Fig. 9 demonstrates that the resulting distance map by the proposed measure provides better view of the feature pixels than that by the conventional gradient refined measure. The distance errors for ten pairs of stereo images using the gradient and LC in the feature pixels is shown in Fig. 10. The distance errors using our LC measure are significantly smaller than those by the conventional gradient measure in the feature pixels.

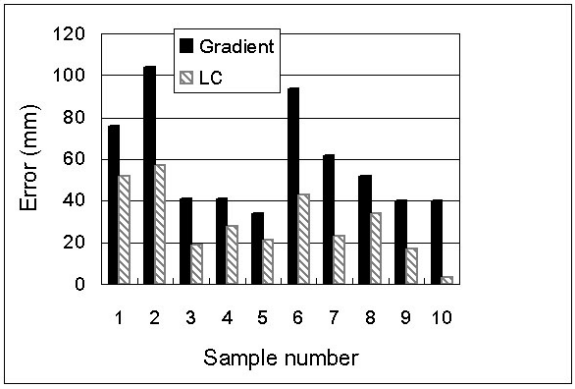

Fig. 10. Distance errors in the feature pixels.

3.3. *Refinement of the measured distance*

Fig. 11 illustrates two linear fits of the number of edge points by our method. For computing the linear fits, we use a plenty of training images. Firstly, the edges of training images are extracted by the Canny edge detector using two sets of thresholds for the gradient, (T_{1_1},T_{2_1}) and (T_{1_2}, T_{2_2}). True distances between the camera and landmarks are measured manually, and are used for ground truth. Then, we make two linear fits between the number of edge points extracted by two sets of thresholds for the gradient and the corresponding true distance. Finally, a shorter

distance τ_1 is estimated by the linear fit in Fig. 11(a), given the number of edge points. Similarly, a longer distance τ_2 is estimated by the linear fit in Fig. 11(b), given the number of edge points. These shorter and longer distances play a major role in the subsequent computation.

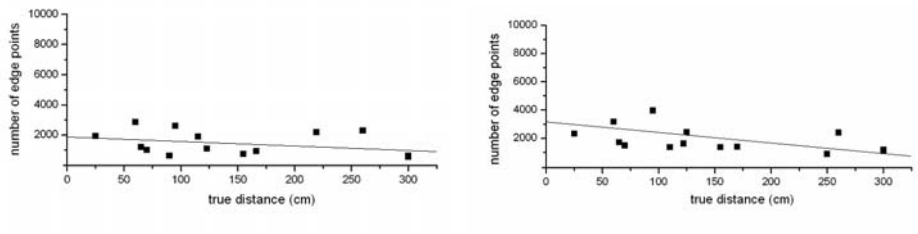

Fig. 11. Two linear fits of the number of edge points for two sets of thresholds for the gradient. (a) $T_{1_1} = 50$ and $T_{2_1} = 150$. (b) $T_{1_2} = 50$ and $T_{2_2} = 250$.

We can estimate the distance between the robot and each landmark by the stereo matching. We use the following threshold elimination function to obtain refined distance by averaging estimated distances.

$$\rho(x) = \begin{cases} x & (if \quad \tau_1 \leq x \leq \tau_2) \\ \tau_2 & (if \quad x > \tau_2) \\ \tau_1 & (if \quad x < \tau_1) \end{cases} \tag{2}$$

Suppose the estimated distances between the robot and features of a landmark are $D = \{d_1, \ldots, d_{N_f}\}$, where N_f is the number of feature pixels in ROI image. The refined distance, d_r, is given by:

$$d_r = \frac{1}{N_f} \sum_{i=1}^{N_f} \rho(d_i) \tag{3}$$

3.4. *Detection of landmarks by a laser scanner*

At the last stage, we compute the distance between the robot and each landmark. In other words, when the robot reaches one of the landmarks, the distance becomes zero and the system can detect it. However, the computed distance based on stereo image still has some error, hence the laser scanner data are applied to improve its estimation. If the refined distance is less than 10cm, we regard that the robot is close enough to the corresponding landmark. Then, the system checks the laser scanner data for still better estimation.

As shown in Fig. 6, the laser scanner has three scanning windows at the right, top and left. During one rotation of the laser scanner, the IR beam passes three windows and provides three distance values. Table 2 gives estimation of landmarks based on the status of the distance measurements. Our robot is designed for the pipes with the diameter ranging from 250 to 350mm. When the robot is moving

inside the sewer pipe, the distance measurement is between 125mm and 175mm. The distance value larger than 175mm is regarded as a distance measure at the landmarks.

Table 2. Estimation of the type of landmarks based on measurements.

Status No.	Distance value larger than 175mm	Estimated landmark type
0	none	no landmark
1	at the top window	manhole
2	at the left window	inlet at the left
3	at the right window	inlet at the right
4	at the top and at the right or left window	manhole with junction
5	at the top, at the right window, and at the left window	robot is outside of the pipe

Fig. 12 illustrates typical places where the KANTARO detects the manhole and inlet in moving through the pipe with diameter 300mm. The rotation starts from the horizontal line (counterclockwisely).

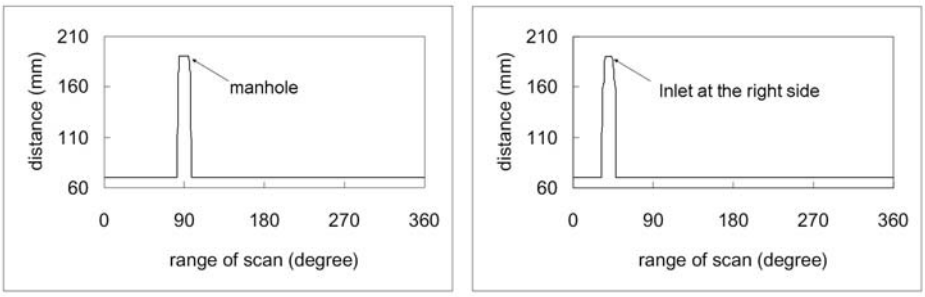

Fig. 12. Typical landmarks detected. (a) The manhole. (b) Inlet at the right side range of scanning.

4. Experimental results

To evaluate the effectiveness of the proposed method, we did a series of experiments by running the KANTARO in the sewer test field (Fig. 13) at FAIS-Robotics Research Institute (RRI). The sewer test field is made by plastic pipes with the diameter ranging from 250 to 300mm.

4.1. *Self localization*

This test demonstrates the accuracy of self localization by capturing stereo images with size of 640×480 pixels such as shown in Fig. 14. We used the lower threshold

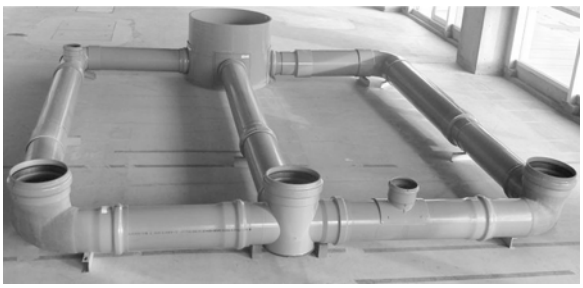

Fig. 13. Sewer test field at RRI.

$T_1 = 50$ and the higher threshold $T_2 = 200$ for edge detection in each ROI images (3.1). Then the distance of feature pixels computed by LC measure (3.2). Next, we used two differents sets of thresholds value for the gradient, ($T_{1_1} = 50$, $T_{2_1} = 150$) and ($T_{1_2} = 50$, $T_{2_2} = 250$) for computing the linear fit, as shown in Fig. 11 (3.3). Finally, the distance error between refind distance, d_r, and the true distance between the camera and a point under consideration in the sewer defined as the following;

$$error = |d_r - d'| \tag{4}$$

Table 3. The percentage of estimation of the distance with error less than 5cm.

Images type	The number of images	Rate(%)
Manhole	32	96.87
Joint	26	88.46
Inlet	12	91.66
Total	70	92.33

Table 3 presents the percentage of estimated distances with error less than 5cm. On the average, about 92% of input sewer images provide the distances with small errors. Although the unstable illumination condition in the real sewer pipe system may effect a large errors in the estimation of the distance. We still have to perform further experiments to fine tune the values of parameters used for edge detection to reduce the errors.

4.2. *Navigation through sewer test field*

This test demonstrates KANTARO's ability in moving through a sewer pipe to the goal by using the proposed method. This experiment requires two basic perceptual abilities: detecting the landmarks and self localization. Both must be executed with high precision, because misperception such as turning action in straight pipe causes damage to KANTARO.

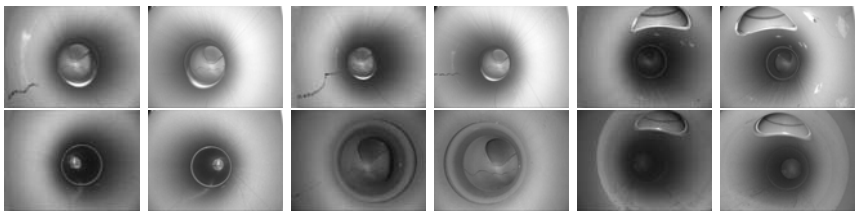

Fig. 14. Samples of stereo images captured by KANTARO during its movement in the sewer test field.

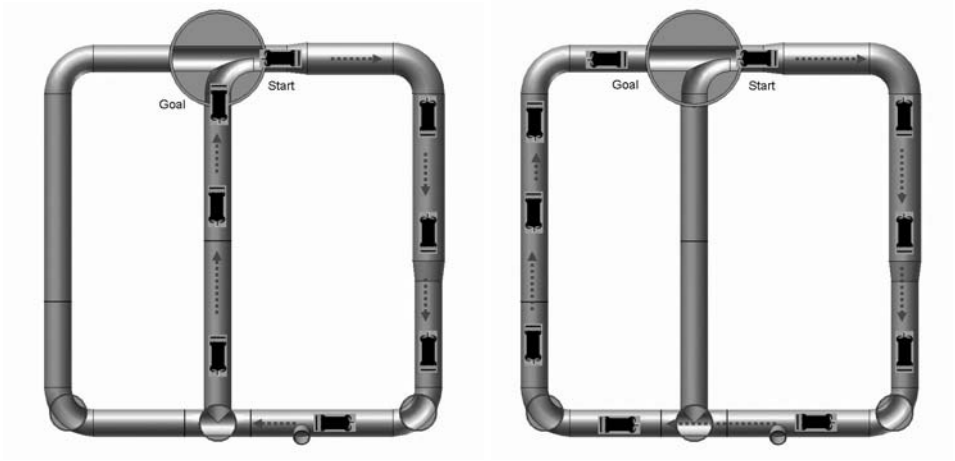

(a) Route 1. (b) Route 2.

Fig. 15. Examples of test navigation routes.

The mission of reaching the goal starting from the initial position is given by a human operator. Fig. 15 provides two different routes in navigation.

When the robot moves along the Route 1, it makes a turning action at the first detected manhole with junction. Due to the position of the laser scanner on KANTARO, the manhole is detected when the robot fully entered into the manhole. At this moment, the robot can't turn, because the front wheel passed the junction entrance. To slove this problem, we modified the action as follows; if the robot enters into the manhole and is to turn it moves backward by 40cm and turns.(Fig. 16).

This mission is successfully achieved in our sewer test field with the maximum speed of 15cm/s. Fig. 17 shows the GUI for navigation during the movement of KANTARO in the sewer test field.

5. Conclusions

We have proposed a method for navigation in sewer pipe systems using the robot platform, KANTARO. Our method uses stereo camera images and laser scanner data for detecting landmarks. It is capable of self localization of the sewer inspec-

Fig. 16. KANTARO turning in the manhole.

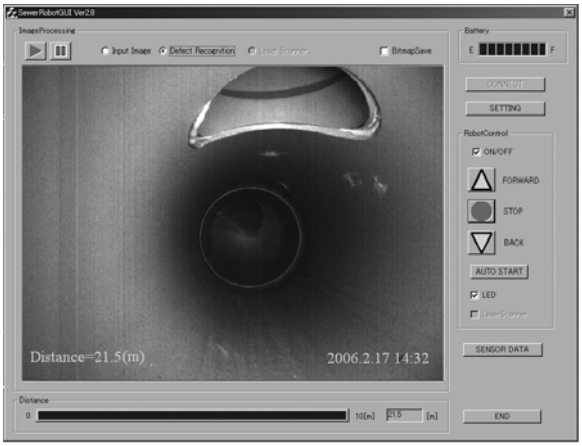

Fig. 17. GUI for navigation.

tion robot, which cannot be done by the conventional methods. The results of self localization experiment shows high performance in providing the appropriate distance. We also design the new mobile laser scanner for KANTARO. The locations of landmarks in sewer pipe system are estimated successfully based on measurements. The laser scanner is fast enough to continuously scan relevant pipe sections in the presence of landmarks, while the KANTARO moves at ordinary inspection speed of up to 15cm/s. Also moving the KANTARO in our sewer test field by using the proposed method was done successfully.

Acknowledgment

This research was supported by the Organization for Small and Medium Enterprises and Regional Innovation, JAPAN (SMRJ).

References

1. Material provided by Sewer System Administration Dept., City of Kitakyushu, Japan.

2. Durbeck, W., "Stand der Eigenkontrollverordnung in den Landern der Bundesrepublik Deutschland aus der Sicht der Industrie," *Dokumentation 4. Int. Kongress Leitungsbau*, Hamburg, Germany, Oct. 1994, pp. 153–166.
3. Keding, M. Riesen, S. van Esch, "Der Zustand der offentlichen Kanalisation in der Bundesrepublik Deutschland. Ergebnisse der ATVUmfrage 1990," *Korrespondenz Abwasser*, Nr.10, 1990, pp. 1148–1153.
4. Rudolph, U., Wellnitz, J., "Zustand und Sanierungsbedarf der Abwasserkanale in den neuen Bundeslandern," *Korrespondenz Abwasser*, 38 Nr.12, 1991, pp. 1625–1630.
5. Hertzberg, J., Kirchner, F., "Landmark-based autonomous navigation in sewerage pipes," *the First EuromicroWorkshop on Advanced Mobile Robots (EUROBOT '96)*, IEEE Press, Los Alamitos, CA, Kaiserslautern, Germany, Oct. 1996.
6. Schonherr, F., Hertzberg, J., Burgard, W., "Probabilistic mapping of unexpected objects by a mobile robot," *the 1999 IEEE/RSJ International Conference on Intelligent Robots and Systems (IROS '99)*, Vol. 1. IEEE Press, Piscataway, NJ, Kyongju, Korea, Oct. 1999.
7. Paletta, L., Rome, E., Pinz, A., "Visual object detection for autonomous sewer robots," *the 1999 IEEE/RSJ International Conference on Intelligent Robots and Systems (IROS '99)*, Vol. 2, IEEE Press, Piscataway, NJ, Kyongju, Korea, Oct. 1999.
8. Campbell, G., Rogers, K., Gilbert, J., "PIRAT - A system for quantitative sewer assessment," *the 12th International No-Dig Conference*, Messe und Congress GmbH, Hamburg, Germany, Sept. 1995.
9. Clarke, T., "The development of an optical triangulation pipe profiling instrument," *Optical 3-D Measurement Techniques III - Applications in inspection, quality control and robotics*, Wichmann, Karlsruhe, Vienna, Oct. 1995.
10. A. Ahrary, L. Tian, S. Kamata, M. Ishikawa, "A cooperative stereo matching algorithm for sewer inspection robots," *the IASTED International Conference on Robotics and Applications*, Cambridge, USA, Oct. 2005, pp. 294–299.
11. D. Scharstein, "Matching images by comparing their gradient fields," in *ICPR*, 1994, Vol.1, pp. 572–575.
12. S. Milan, H. Vaclav and B. Roger, *Image Processing, Analysis, and Machine Vision*, pp. 448–502, Thomson Press, 2002.
13. J. Canny, "A Computational approach to edge detection," *IEEE Transactions on Pattern Analysis and Machine Intelligence*, Vol 8, No. 6, Nov 1986.
14. A. Ahrary, A. Nassiraei, M. Ishikawa, "A tudy of an autonomous mobile robot for sewer inspection system," *Proc. of the 11th Int. Symposium on Artificial Life and Robotics (AROB'06)*, Oita, Japan, Jan.2006.
15. P. Anandan, "A computational framework and an algorithm for the measurement of visual motion," *IJCV*, 2(3): 283-310, 1989.